Optics Letters

Omnidirectional broadband phase modulation by total internal reflection

ZHIDA LIU,[1,†] JIAYAO LIU,[1,†] SICHAO QU,[2] AND ZHAONA WANG[1,*]

[1]Department of Physics, Applied Optics Beijing Area Major Laboratory, Beijing Normal University, Beijing 100875, China
[2]Department of Physics, The Hong Kong University of Science and Technology, Hong Kong SAR 999077, China
[†]These authors contributed equally to this work.
*zhnwang@bnu.edu.cn

Received 6 September 2023; revised 1 October 2023; accepted 7 October 2023; posted 11 October 2023; published 26 October 2023

Phase modulation plays a crucial role in shaping optical fields and physical optics. However, traditional phase modulation techniques are highly dependent on angles and wavelengths, limiting their applicability in smart optical systems. Here, we propose a first-principle theory for achieving constant phase modulation independent of incident angle and wavelength. By utilizing a hyperbolic metamaterial and engineering-specific optical parameters, different reflective phase jumps are achieved and tailored for both transverse electric (TE) and transverse magnetic (TM) waves. The aimed reflection phase difference between TE and TM waves can be thus achieved omnidirectionally and achromatically. As an example, we propose a perfect omnidirectional broadband reflection quarter wave plate. This work provides fundamental insights into manipulating optical phases through optical parameter engineering.

https://doi.org/10.1364/OL.505024

Phase modulation plays a key role in reshaping the wavefront of optical waves and finds broad practical applications in various branches of industry and scientific fields. Traditional photonic devices rely on phase modification to achieve wavefront modification and beam shaping. To further tailor the phase difference between the two orthogonal polarized components, polarization states of waves can be manipulated by separately adjusting the accumulated phase. Typically, phase modification is obtained by using transmission and/or reflection processes. In particular, the transmission phase modification strategy is commonly employed in conventional optical elements. For example, traditional wave plates utilize birefringent crystals with specific thicknesses to alter the polarization states of light. The emergence of metamaterials with unique parameters has led to novel opportunities for exploring phenomena such as negative refraction, subwavelength focusing, and even the concept of "invisibility cloaks" [1–4]. However, traditional transmission photonic devices face substantial challenges in fabrication technology and the realization of smart devices [5]. In order to reduce the size of the smart photonic elements and enable versatile wavefront control applications, the concept of metasurface with interfacial phase discontinuity has been utilized to reshape the wavefront [6–11] using the 2π periodicity of phase variation. Based on the transmissive phase modulation strategy, plenty of photonic elements have been developed to meet various functionalities in different application scenarios. However, the effectiveness of transmission phase modulation is highly dependent on incidental wavelength and optical thickness [12,13], resulting in constraints on working wavelength bandwidths and specific demands for incident angles [14]. Consequently, there exists a strong demand for the advancement of an intelligent phase control theory capable of facilitating the design of novel photonic devices with extremely broad wavelength and angle bandwidths.

An alternative approach involves the help of reflective phase modulation photonic devices. Fresnel's rhomb can give a relative reflection phase difference (RPD) of 90° through two successive total internal reflections at specific angles [15]. However, the phase jumps of transverse electric (TE) waves and transverse magnetic (TM) waves vary with the incident angle, as well as the RPD when total internal reflection happens at the interface of the traditional media [15]. Recently, hyperbolic metamaterials (HMMs) have attracted broad interests due to their unique dispersion relations particularly with an open hyperbolic equifrequency contour [1,16–21]. HMMs provide intriguing possibilities for the development of omnidirectional photonic devices by tuning the shape of the hyperbolic dispersion [22]. In our previous work, we propose a theory that enables the realization of a perfect polarization beam splitter with an exceptionally broad frequency and angle bands without energy loss [23]. This serves as a promising foundation for further developing a phase modulation theory with high efficiency and extremely broad bands based on HMMs.

In this work, we propose a novel reflective phase modulation theory to design highly efficient photonic devices with extremely broad bands in angles and wavelengths. Based on the total internal reflection at the interface of isotropic medium and the HMM, a constant phase jump phenomenon that is independent on incident angle and wavelength for both TE and TM waves is observed. This unique phenomenon indicates a constant RPD, laying the foundation for a reflective phase modulation theory to design high-efficiency photonic devices with broad bands in angle and wavelength. As an example, we propose a perfect total internal reflection quarter wave plate (QWP). This theoretical work provides valuable guidance for designing phase

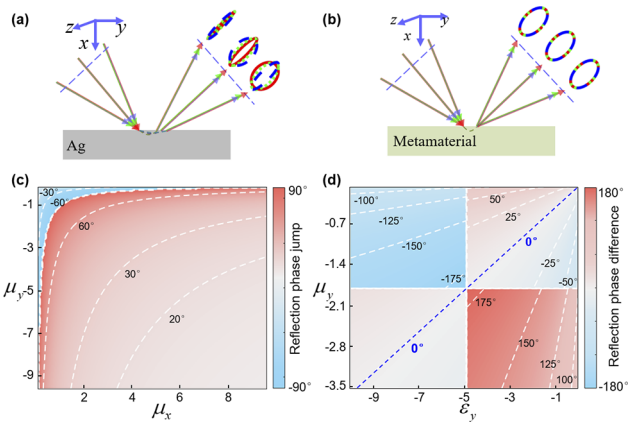

Fig. 1. (a), (b) Schematic diagram of total internal reflection of a linear polarization beam at a vacuum–metal interface (a) and at the vacuum–metamaterial interface with a constant phase jump (b). (c) The reflection phase jump for TE waves varies with μ_x and μ_y at $\mu_1 = 1$. (d) The reflection phase difference between TE and TM waves varies with ε_y and μ_y at $\varepsilon_1 = 1.7$, $\mu_1 = 1$, $\varepsilon_x = 0.586$, $\varepsilon_z = 3$, $\mu_x = 0.567$, and $\mu_z = 2.9$.

modulation devices with broadband operation and minimal loss, offering a great potential for applications in complex optical systems.

In the traditional total internal reflection process, the RPD between the TE and TM waves varies with the incident angle and wavelength when a spatial wave packet with linear polarization is incident on the vacuum–metal interface [Fig. 1(a)]. As a result, the polarization states of the reflected waves vary with the position on the observation plane. To achieve a consistent polarization state, a constant RPD is required with the help of metamaterials, regardless of the incident angle and wavelength [Fig. 1(b)]. For this purpose, we consider an interface between the isotropic dielectric medium with permittivity ε_1 and permeability μ_1 and anisotropic metamaterial characterized by principal tensorial permittivity ($\hat{\varepsilon}$) and permeability ($\hat{\mu}$), as shown in Fig. 1(b). The x and y axes are parallel to the optical axis of the anisotropic materials with x axis normal to the interface. The incident beams are incidental in the xOy plane. The principal tensorial permittivity and permeability have the following forms [16] of $\hat{\varepsilon} = \varepsilon_0\varepsilon_i$ and $\hat{\mu} = \mu_0\mu_i$ $(i = x, y, z)$ with ε_i and μ_i $(i = x, y, z)$ being the relative permittivity and permeability components, respectively.

From Maxwell's equations, the dispersion relation of the anisotropic medium can be derived as [23] $\frac{k_x^2}{\varepsilon_y} + \frac{k_y^2}{\varepsilon_x} - \mu_z k_0^2 = 0$ for TM waves and $\frac{k_x^2}{\mu_y} + \frac{k_y^2}{\mu_x} - \varepsilon_z k_0^2 = 0$ for TE waves. Here, $k_i (i = x, y)$ is the modulus of the wave vector component, and k_0 is the wave number in vacuum. Indeed, for TM and TE waves, the dispersion relation takes the form of a hyperbolic shape when $\varepsilon_y\varepsilon_x<0$ and $\mu_z>0$ for TM waves and $\mu_y\mu_x<0$ and $\varepsilon_z>0$ for TE waves. When the dispersion curves of incident medium 1 and the HMM do not intersect, a total internal reflection phenomenon occurs, causing all incident waves from medium 1 to be fully reflected. To achieve this total internal reflection, the optical parameters of the metamaterial must satisfy specific conditions [23]. The required relation is of $\varepsilon_y\mu_z<0$ and $\varepsilon_y\mu_z \le \frac{\varepsilon_y}{\varepsilon_x}\varepsilon_1\mu_1$ for TM waves, and the condition of $\mu_y\varepsilon_z<0$ and $\mu_y\varepsilon_z \le \frac{\mu_y}{\mu_x}\varepsilon_1\mu_1$ for TE waves. For the incident TM and TE waves from medium 1 into HMM, reflection coefficients at the interface are written as [23]

$$r_{\mathrm{TM}} = \frac{k_{1x}\varepsilon_y - k_x\varepsilon_1}{k_{1x}\varepsilon_y + k_x\varepsilon_1}, \tag{1a}$$

$$r_{\mathrm{TE}} = \frac{k_{1x}\mu_y - k_x\mu_1}{k_{1x}\mu_y + k_x\mu_1}. \tag{1b}$$

Here, k_{1x} and k_x represent the normal components of the wave vector for incident waves and refracted waves, respectively. During total internal reflection, the refracted waves in the anisotropic metamaterial have complex wave numbers, leading to rapid decay. To account for this decay property, we define a real number $\alpha = \mathrm{Im}(k_x)$. The phase jumps of TE and TM waves during the total internal reflection can be calculated using Eq. (1) and are given as follows:

$$\phi_{\mathrm{TM}} = \tan^{-1}\left(\frac{-2\alpha_{\mathrm{TM}}\varepsilon_1\varepsilon_y k_{1x}}{k_{1x}^2\varepsilon_y^2 - \alpha_{\mathrm{TM}}^2\varepsilon_1^2}\right), \tag{2a}$$

$$\phi_{\mathrm{TE}} = \tan^{-1}\left(\frac{-2\alpha_{\mathrm{TE}}\mu_1\mu_y k_{1x}}{k_{1x}^2\mu_y^2 - \alpha_{\mathrm{TE}}^2\mu_1^2}\right). \tag{2b}$$

To achieve the phase modulation over an extremely broad angle and wavelength ranges, the reflection coefficient needs to remain constant regardless of incident angles and wavelengths. Mathematically, the phase jump ϕ_i (i = TM or TE) should satisfy $\partial\phi_i/\partial k_y = 0$ (i = TM or TE) for a broad angle band and $\partial\phi_i/\partial k_0 = 0$ (i = TM or TE) for a broad spectral band. We define the parameter $\gamma_i = k_{1x}^2/\alpha_i^2$ (i = TM or TE). The conditions of $\partial\phi_i/\partial k_y = 0$ and $\partial\phi_i/\partial k_0 = 0$ will be satisfied at $\partial\gamma_i/\partial k_y = 0$ and $\partial\gamma_i/\partial k_0 = 0$ if $\hat{\varepsilon}$ and $\hat{\mu}$ are wavelength independent. From dispersion relation of the HMM, γ is expressed as $\gamma_{\mathrm{TM}} = -\frac{\varepsilon_x(\varepsilon_1\mu_1 k_0^2 - k_y^2)}{\varepsilon_y(\varepsilon_x\mu_z k_0^2 - k_y^2)}$ and $\gamma_{\mathrm{TE}} = -\frac{\mu_x(\varepsilon_1\mu_1 k_0^2 - k_y^2)}{\mu_y(\mu_x\varepsilon_z k_0^2 - k_y^2)}$. By carefully selecting the optical parameters, we can ensure γ remains constant regardless of k_y and k_0 when the optical parameters satisfy $\mu_x\varepsilon_z = \varepsilon_1\mu_1$ for TE waves and $\mu_z\varepsilon_x = \varepsilon_1\mu_1$ for TM waves. Thus, to achieve a constant reflective phase jump with total internal reflection, the relative permittivity and relative permeability of the anisotropic metamaterial should satisfy the following relationships:

$$\mathrm{TM}: \varepsilon_y\mu_z \le \frac{\varepsilon_y}{\varepsilon_x}\varepsilon_1\mu_1,\ \mu_z\varepsilon_x = \varepsilon_1\mu_1,\ \varepsilon_y<0 \text{ and } \mu_z>0, \tag{3a}$$

$$\mathrm{TE}: \mu_y\varepsilon_z \le \frac{\mu_y}{\mu_x}\varepsilon_1\mu_1,\ \mu_x\varepsilon_z = \varepsilon_1\mu_1,\ \mu_y<0 \text{ and } \varepsilon_z>0. \tag{3b}$$

Under these requirements, γ degenerates to $\gamma_{\mathrm{TM}} = -\varepsilon_x/\varepsilon_y$ and $\gamma_{\mathrm{TE}} = -\mu_x/\mu_y$ as a constant independent on wavelength and incident angle. The corresponding phase jump for the reflected TM and TE waves are separately given by Eq. (4) as

$$\phi_{\mathrm{TM}} = \tan^{-1}\left(\frac{2\varepsilon_1\varepsilon_y\sqrt{-\varepsilon_x/\varepsilon_y}}{\varepsilon_x\varepsilon_y + \varepsilon_1^2}\right), \tag{4a}$$

$$\phi_{\mathrm{TE}} = \tan^{-1}\left(\frac{2\mu_1\mu_y\sqrt{-\mu_x/\mu_y}}{\mu_x\mu_y + \mu_1^2}\right). \tag{4b}$$

This means all incident TE and TM waves will be totally reflected with a constant phase jump determined solely by the optical parameters of HMM. The constant phase jump at total reflection is fundamentally different from traditionally totally internal reflection, where the phase jump varies with incident angle [15]. This unique characteristic enables synchronous phase modulation for spatial wave packets within a

specific spectral bandwidth. Additionally, this reflection does not alter the polarization state distribution of the incident optical field, distinguishing it from mirror reflection. Furthermore, the Goos–Hänchen shift at the designed interface is consistently zero for all incident waves, as calculated by $\Delta GH = -\frac{d\phi_i}{kd\theta}$ [24], setting it apart from traditional total internal reflection [25–27].

Notably, the constant phase variation can be individually tuned by adjusting the optical parameters for the TE and TM waves. According to Eqs. (4a) and (4b), the phase jump for the TE waves and TM waves individually covers the range of $(-\pi/2, \pi/2)$. As shown in Fig. 1(c), TE waves demonstrate a set of phase jump with changing μ_x and μ_y as expected. A jump behavior of phase jump from –90° to 90° appears at $\mu_x\mu_y = -1$. The reflection phase difference between TE and TM waves, a result of phase jump summation, is constant within the range of $(-\pi, \pi)$ by tailoring the optical constants as shown in Fig. 1(d). This feature is ideal for phase modulation devices. When the constant phase difference is zero [the blue line in Fig. 1(d)], polarization-independence photonic devices can be achieved. Alternatively, a total internal reflection wave plate with broad spectral and angle bands can be obtained when a non-zero phase difference is achieved. It should be pointed out that the jump phenomenon at $\varepsilon_y = -4.93$ and $\mu_y = -1.76$ is induced by the singular point in the reflection phase jump Eqs. (4a) and (4b).

As an example, we demonstrate a perfect total internal reflection QWP with broad angle and wavelength bands theoretically. The condition for a $\pi/2$ phase jump requires $\tan(\phi_{TE})\tan(\phi_{TM}) = -1$. Consider a special scenario where TE and TM waves have similar dispersion relations under the condition of $\mu_i = \beta\varepsilon_i (i = x, y, z)$ with a constant β to ensure total internal reflection with a constant phase jump. We obtain the formula $\varepsilon_x\varepsilon_y = \frac{-\beta_2 \pm \sqrt{\beta_2^2 - 4\beta^2}}{2\beta^2}$ with $\beta_2 = \beta^2 - 4\beta + 1$. Therefore, the requirements for a perfect omnidirectional and broadband QWP are given as $\varepsilon_x = \frac{1}{\beta\varepsilon_z}$, $\varepsilon_y = \frac{-\beta_2\varepsilon_z \pm \sqrt{\beta_2^2\varepsilon_z^2 - 4\beta^2\varepsilon_z^2}}{2\beta}$, $\mu_x = \frac{1}{\varepsilon_z}$, $\mu_y = \frac{-\beta_2\varepsilon_z \pm \sqrt{\beta_2^2\varepsilon_z^2 - 4\beta^2\varepsilon_z^2}}{2}$, and $\mu_z = \beta\varepsilon_z$. Parameter β is in the ranges of $(0, 3 - 2\sqrt{2}]$ and $[3 + 2\sqrt{2}, \infty)$.

The performances of the designed perfect omnidirectional and broadband QWP are demonstrated through finite element simulation in Fig. 2, by calculating the reflection phase jump of TE waves and TM waves at the interface of vacuum and HMM. The Gaussian TE waves [Figs. 2(a) and 2(b)] and TM waves [Fig. 2(c)] are totally reflected back at the incident angle θ_{in} of 45° with minimal loss. When a linearly polarized Gaussian beam is incident on the QWP, the phase difference between the magnetic field components H_z and H_y of the reflected Gaussian beam is fitted as about $\pi/2$, representing the RPD between the TM waves and TE waves. Figure 2(d) demonstrates the calculated RPD of the TM and TE Gaussian beams under different θ_{in} from 10° to 80°, indicating a broadband modulation in angle. At $\theta_{in} = 30°$ and $\theta_{in} = 45°$, the designed QWP almost demonstrates a $\pi/2$ RPD between the TM and TE Gaussian beams with different wavelengths from 200 nm to 1100 nm in Fig. 2(e). The small difference between the calculated RPD and $\pi/2$ might be induced by the limit mesh accuracy. The results verify the excellent broad wavelength and angular band merits of the designed perfect QWP.

In Fig. 3, we investigate the effect of medium dispersion on the performances of the designed QWP. Considering that the real permittivity and permeability are often functions of wavelength, the permittivity component ε_z of the metamaterial is chosen as the Drude model $\varepsilon(\omega) = 1 - \frac{\omega_p^2}{\omega^2 + i\gamma\omega}$ with the wave frequency

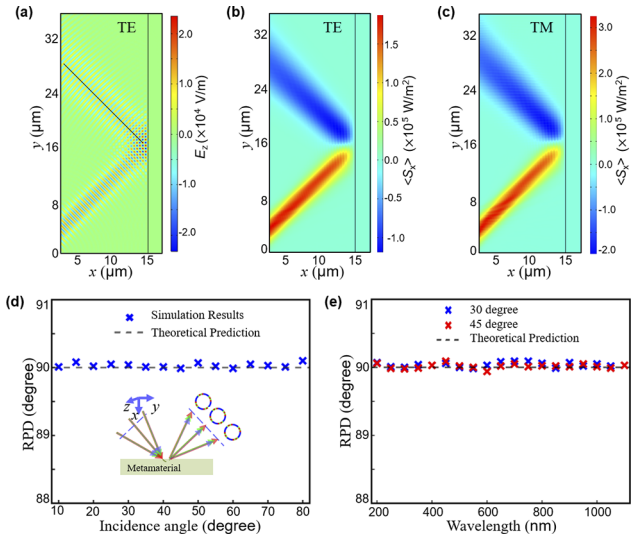

Fig. 2. Performances of the designed perfect quarter wave plate (QWP). (a), (b) E_z (a) and x component of time-averaged power flow $< S_x >$ (b) distributions when the TE waves are incident on the QWP at θ_{in} =45°. (c) $< S_x >$ for the TM waves at θ_{in} =45°. (d, e) The RPD between TM and TE waves varies with the incident wavelength at $\theta_{in} = 30°$ and 45° (d) and with θ_{in} for a 600 nm beam. The waist of the Gaussian beams is 2.0 μm. The optical parameters are $\varepsilon_x = 1/6$, $\varepsilon_y = -2/3$, $\varepsilon_z = 1$, $\mu_x = 1$, $\mu_y = -4$, and $\mu_z = 6$.

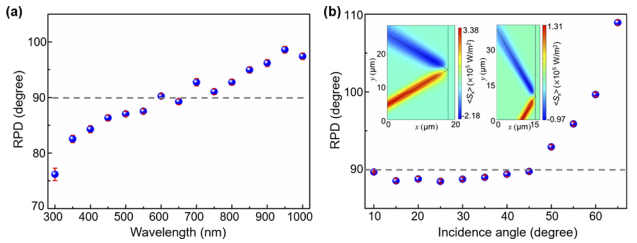

Fig. 3. The effect of medium dispersion on the RPD of the designed QWP. (a) RPD of the designed QWP varies with wavelength at θ_{in} =45°. (b) RPD of the designed QWP varies with θ_{in} at a wavelength of 600 nm. The insets are $< S_x >$ distributions at θ_{in} =30° (left) and θ_{in} =60° (right). The error bar is simulated by the H_z and H_y curves.

ω, the plasma frequency $\omega_p = 3.87 \times 10^{15}$ rad/s, and the damping constant $\gamma = 9.8 \times 10^{15}$ rad/s [28]. Figure 3(a) demonstrates the effect of dielectric dispersion on the RPD of the designed omnidirectional broadband reflection QWP. The RPD almost maintains at 90° for the different Gaussian beams with the wavelength in the range [450, 850] nm, demonstrating a broadband property. For an incident Gaussian beams with a wavelength of 600 nm, the RPD is still around 90° when the incidental angle is from 10° to 50° in Fig. 3(b). The time-averaged power flow component $< S_x >$ distributions indicate that the Gaussian waves are almost totally reflected, meaning a neglectable loss. The result indicates that the perfect omnidirectional broadband QWP might be able to be fabricated using dispersive materials, which opens up possibilities for its implementation and design in practical applications.

In the structure design of the proposed HMMs, the modulation of TM and TE waves can be achieved separately. Electric hyperbolic dispersion metamaterials are already relatively mature [16]. To achieve negative dielectric tensor elements that satisfy the condition of Eq. (3a), metal films or metal wire arrays can be integrated with dielectric materials [29]. On the other hand, HMM for TE waves, controlled by Eq. (3b), can be realized using Mie resonance or split-ring resonators [30,31]. Additionally, the phase modulation elements controlled by the topological chiral media have been experimentally demonstrated, indicating chiral media as an alternative choice for the reflected phase modulation elements [32,33]. By carefully selecting and adjusting these modification parameters, it is possible to create practical and efficient reflection phase modulation structures for both TM and TE waves, which provide potential guidance for the actual implementation in real-world applications.

In this work, we demonstrated a constant RPD phenomenon at the dielectric–metamaterial interface. We propose a novel reflection phase modulation theory, based on the generalized Fresnel formulas for anisotropic metamaterials, which enables the design of high-efficiency photonic devices with broad angle and wavelength bands, overcoming the thickness restriction. By carefully adjusting the dispersion properties of HMM, we can achieve a constant RPD for TE and TM waves, independent of incident angle and wavelength. The constant RPD allows for a precise control of the reflected wavefront, making it possible to design efficient photonic devices with versatile applications. As an example, we designed a perfect omnidirectional and broadband QWP that promises a constant $\pi/2$ RPD between the TM and TE waves at any incident angle and wavelength. We validated the performance of the designed perfect QWP through finite element simulations, and we also investigated the impact of material wavelength dispersion on its performance. One key advantage of our proposed HMMs is their ability to act as meta-atoms, enabling local manipulation of photon phase and flexible modification of electromagnetic wavefronts through total internal reflection down to the wavelength scale. This property may deepen one's understanding of total internal reflection and open up new possibilities for designing phase modulation-based photonic devices with unprecedented functionalities and performance. Our work lays the theoretical foundation for the design of a wide range of phase modulation-based photonic devices and may open the era of total internal reflection photonics.

Funding. National Natural Science Foundation of China (61975018, 92150109); Beijing Municipal Science and Technology Commission, Administrative Commission of Zhongguancun Science Park (Z221100002722019); Fok Ying Tung Graduate School of the Hong Kong University of Science and Technology.

Disclosures. The authors declare no conflicts of interest.

Data availability. Data underlying the results presented in this paper are not publicly available at this time but may be obtained from the authors upon reasonable request.

REFERENCES

1. L. Ferrari, C. H. Wu, D. Lepage, *et al.*, Prog. Quant. Electron. **40**, 1 (2015).
2. J. B. Pendry, D. Schurig, and D. R. Smith, Science **312**, 1780 (2006).
3. Z. J. Wang, F. Cheng, T. Winsor, *et al.*, Nanotechnology **27**, 412001 (2016).
4. U. Leonhardt, Science **312**, 1777 (2006).
5. C. M. Soukoulis and M. Wegener, Nat. Photonics **5**, 523 (2011).
6. F. Ding, Z. X. Wang, S. L. He, *et al.*, ACS Nano **9**, 4111 (2015).
7. N. F. Yu, P. Genevet, M. A. Kats, *et al.*, Science **334**, 333 (2011).
8. X. J. Ni, A. V. Kildishev, and V. M. Shalaev, Nat. Commun. **4**, 2807 (2013).
9. F. Aieta, P. Genevet, M. A. Kats, *et al.*, Nano Lett. **12**, 4932 (2012).
10. X. J. Ni, S. Ishii, A. V. Kildishev, *et al.*, Light: Sci. Appl. **2**, e72 (2013).
11. X. J. Ni, N. K. Emani, A. V. Kildishev, *et al.*, Science **335**, 427 (2012).
12. Z. L. Han, S. Ohno, Y. Tokizane, *et al.*, Opt. Lett. **43**, 2977 (2018).
13. B. A. Yang, W. M. Ye, X. D. Yuan, *et al.*, Opt. Lett. **38**, 679 (2013).
14. L. A. Gubanova and E. S. Putilin, J. Opt. Technol. **79**, 102 (2012).
15. M. W. Born, *Principles of Optics*, 7th ed. (Cambridge University Press, 1999).
16. A. Poddubny, I. Iorsh, P. Belov, *et al.*, Nat. Photonics **7**, 948 (2013).
17. M. V. Davidovich, Phys.-Usp. **62**, 1173 (2019).
18. Z. W. Guo, H. T. Jiang, and H. Chen, J. Appl. Phys. **127**, 071101 (2020).
19. F. Wu, G. Lu, Z. W. Guo, *et al.*, Phys. Rev. Appl. **10**, 064022 (2018).
20. A. Aigner, J. M. Dawes, S. A. Maier, *et al.*, Light: Sci. Appl. **11**, 9 (2022).
21. F. Wu, M. Y. Chen, and S. Y. Xiao, Opt. Lett. **47**, 2153 (2022).
22. F. Wu, G. Lu, C. H. Xue, *et al.*, Appl. Phys. Lett. **112**, 041902 (2018).
23. Z. D. Liu, J. Q. Guo, B. Y. Tian, *et al.*, Opt. Express **27**, 7673 (2019).
24. K. Artmann, Annalen der Physik **437**, 87 (1948).
25. X. Li, P. Wang, F. Xing, *et al.*, Opt. Lett. **39**, 5574 (2014).
26. F. Goos and H. Hanchen, Ann. Phys. **436**, 333 (1947).
27. R. U. Din, X. D. Zeng, I. Ahmad, *et al.*, Appl. Phys. Lett. **114**, 161902 (2019).
28. M. A. Ordal, R. J. Bell, R. W. Alexander, *et al.*, Appl. Opt. **24**, 4493 (1985).
29. C. R. Simovski, P. A. Belov, A. V. Atrashchenko, *et al.*, Adv. Mater. **24**, 4229 (2012).
30. F. Martin, J. Bonache, F. Falcone, *et al.*, Appl. Phys. Lett. **83**, 4652 (2003).
31. C. W. Lan, K. Bi, B. Li, *et al.*, Opt. Express **21**, 29592 (2013).
32. X. X. Wang, Z. W. Guo, J. Song, *et al.*, Nat. Commun. **14**, 3040 (2023).
33. J. Wang, H. Tian, S. Li, *et al.*, Opt. Lett. **45**, 1276 (2020).